



INSTITUT DE FRANCE
Académie des sciences

Comptes Rendus

Géoscience

Sciences de la Planète


Mesut Gündüz, Ayla Bozdağ, Ali Ferat Bayram, Ali Bozdağ, Kürşad Asan
and Paul Sardini

**Water-rock interaction in the geothermal systems related to post-collision zone
volcanism: A case study based on multivariate statistical analysis from the Kavak
geothermal field (Konya, Turkey)**

Volume 355 (2023), p. 311-329

Published online: 18 December 2023

<https://doi.org/10.5802/crgeos.249>

 This article is licensed under the
CREATIVE COMMONS ATTRIBUTION 4.0 INTERNATIONAL LICENSE.
<http://creativecommons.org/licenses/by/4.0/>



*Les Comptes Rendus. Géoscience — Sciences de la Planète sont membres du
Centre Mersenne pour l'édition scientifique ouverte*

www.centre-mersenne.org

e-ISSN : 1778-7025



Research article — Hydrology, hydrogeology

Water–rock interaction in the geothermal systems related to post-collision zone volcanism: A case study based on multivariate statistical analysis from the Kavak geothermal field (Konya, Turkey)

Mesut Gündüz^{Ⓢ,* , a}, Ayla Bozdağ^b, Ali Ferat Bayram^b, Ali Bozdağ^b, Kürşad Asan^b and Paul Sardini^c

^a Graduate School of Natural and Applied Sciences, Muğla Sıtkı Koçman University, TR-48000, Muğla, Turkey

^b Geological Engineering Department, Konya Technical University, TR-42250, Konya, Turkey

^c Institut de Chimie des Milieux et Matériaux de Poitiers (IC2MP), CNRS, (E2-HydrASA), Université de Poitiers, F-86073, Poitiers, France
E-mail: mesutgunduz24@hotmail.com (M. Gündüz)

Abstract. Water–rock interaction is the focus of geothermal energy studies and can be documented by traditional geochemical methods such as ion ratio method and hydrogeochemical modelling etc. Statistical approaches are also vital for the quantitative models, and mainly combined with the traditional methods. In this study, we re-evaluate the published data, including water chemistry and volcanic and metamorphic whole-rock geochemistry from the Kavak geothermal field (Konya, Turkey) by using multivariate statistical analysis (e.g. factor analysis and clustering analysis) to research possible interaction between the thermal waters and surrounding rocks.

The Kavak geothermal field (KGF) overlies a metamorphic basement composed of the Paleozoic metacarbonates and metaclastic rocks, yet is located near the Erenlerdağ–Alacadağ volcanic complex (ErAVC). An example of unimodal orogenic volcanism in an extensional geodynamic setting, the Neogene ErAVC is composed of widespread high-K calcalkaline andesite to rhyodacite lavas with enclaves and their pyroclastic counterparts. The Kavak geothermal field covers a small area (~7.5 km²) and lies along the Seydişehir fault zone in the southeast of the ErAVC. The Kavak thermal waters are meteoric in origin and peripheral waters (Ca–Na–HCO₃) in the geothermal system related to the orogenic volcanism. The Kavak thermal waters are characterised by high K⁺ and Na⁺ cations, and low pH (between 6.4–6.9 pH) values relative to the cold waters around the KGF. Two types of thermal waters were identified in the KGF based on the slight difference in their hydrochemistry and discharge temperature. The first type thermal water (~22 °C) has higher TDS and Cl/Br ratio and lower dissolved silica and Br content relative to the second type of water (up to 45 °C). The chemical relationship between the KGF and high-K ErAVC is clearly seen in the cation-based diagrams. Multivariate statistical analysis confirms that first type and second type thermal waters identified

* Corresponding author.

based on their hydrochemistry formed two separate statistical groups, and suggests that the chemistry of the KGF waters was mainly controlled by the composition of the ErAVC rather than those of the basement metamorphic rocks as a result of water–rock interaction.

Keywords. Kavak geothermal field, Water–rock interaction, Hydrogeochemistry, Data analysis of the thermal waters, Silicate weathering.

Manuscript received 20 May 2023, revised 17 November 2023, accepted 1 December 2023.

1. Introduction

Water–rock interaction (WRI), one of the most important factors that deeply control the geochemistry of thermal waters is a prime interest in geothermal energy studies. Although this phenomenon has been known for many years by earth scientists, its nature has always been debated [Wohletz and Heiken, 1992]. WRI encompasses primarily three types of reactions, namely adsorption, dissolution, and precipitation that take place at the mineral–fluid interfaces [Teng, 2005]. WRI can be documented by theoretical, experimental, field, and laboratory studies, based mainly on the geochemical and isotopic data. After the acquisition data, WRI can be studied by traditional methods such as ion ratio method and hydrogeochemical modelling software (e.g. PHREEQC). Multivariate statistical analysis techniques have recently been combined with these methods. Factor analysis and principal component analysis (PCA) are commonly used multivariate statistical analysis techniques [Poznanović-Spahić *et al.*, 2023, Zhang *et al.*, 2022]. These statistical methods are useful to analyse all parameters in a large dataset as a whole, which allows practically to screen, reduce and classify the data. Compared to the traditional methods, they serve as a more powerful tool on the deciphering origin, interaction with the rocks and circulation pathway of thermal waters [Hao *et al.*, 2020, Yidana *et al.*, 2012].

The Kavak geothermal field (KGF) is a fault-controlled thermal system of meteoric origin located in the southwest of the Erenlerdağ–Alacadağ volcanic complex [Bayram, 1992, Bozdağ, 2016, Burçak *et al.*, 2002, Davraz *et al.*, 2022a,b, Göçmez *et al.*, 2005, Göçmez and Şen, 1998] (Figures 1 and 2). Using traditional methods, previous studies emphasised that water–rock interactions and decomposition processes, and argued the interaction between the thermal waters and metamorphic basement rocks played an important role in the KGF [Bozdağ, 2016, Davraz *et al.*, 2022a,b, Karaisaoğlu and Orhan, 2018]. However, the possible interaction between the

thermal waters and volcanic rocks of the Erenlerdağ–Alacadağ volcanic complex (e.g. ErAVC) as a geothermal heat source in the KGF was not evaluated in the previous studies. Hence, we here reprocess the published geochemical data from the thermal waters, volcanic and metamorphic rocks in the KGF using multivariate statistical analysis (e.g. factor analysis and clustering analysis) and evaluate whether interactions between the Kavak thermal waters and volcanic rocks in the ErAVC play a decisive role in water chemistry.

2. Geological and hydrogeological setting

Located in the Central Taurus, the KGF is in the Beyşehir Basin characterised by a graben-like structure, including several units with different stratigraphic, lithologic, tectonic, volcanic, and metamorphic features (Figure 2). The Beyşehir Basin, which controls the morpho-tectonic structure of the Kavak geothermal field, is mostly related to the northwest–southeast trending (sub) parallel normal faults. The Mio-Pliocene fluvio-lacustrine deposits around the KGF are proof of the fault-controlled intermontane basin in the region [Koç *et al.*, 2017, 2018]. In addition, this graben system (i.e. Beyşehir Basin) is surrounded by the Taurus belt from the SW and the Afyon zone from the NE. It is also separated from the Konya graben in the north. The morpho-tectonic structures of the study area and seismic activities in recent years indicate that the faults in the region (i.e. Abazdağı, Beyşehir, and Seydişehir fault zones, etc.) are a part of the active-neotectonic structure [Aksoy, 2019]. The Kavak geothermal field is an example of the fault-controlled spring system [Keegan-Treloar *et al.*, 2022] and thermal water springs of the KGF discharge along a fault in the north (e.g. TS4 and TS5 thermal waters) and fault in the south (e.g. TS1, TS2 and TS3 thermal waters) parallel to the Seydişehir Fault Zone (Figures 2, 3). The southern fault acts actually as a structural (semi) barrier, leading to the existence of two types of thermal waters in terms of

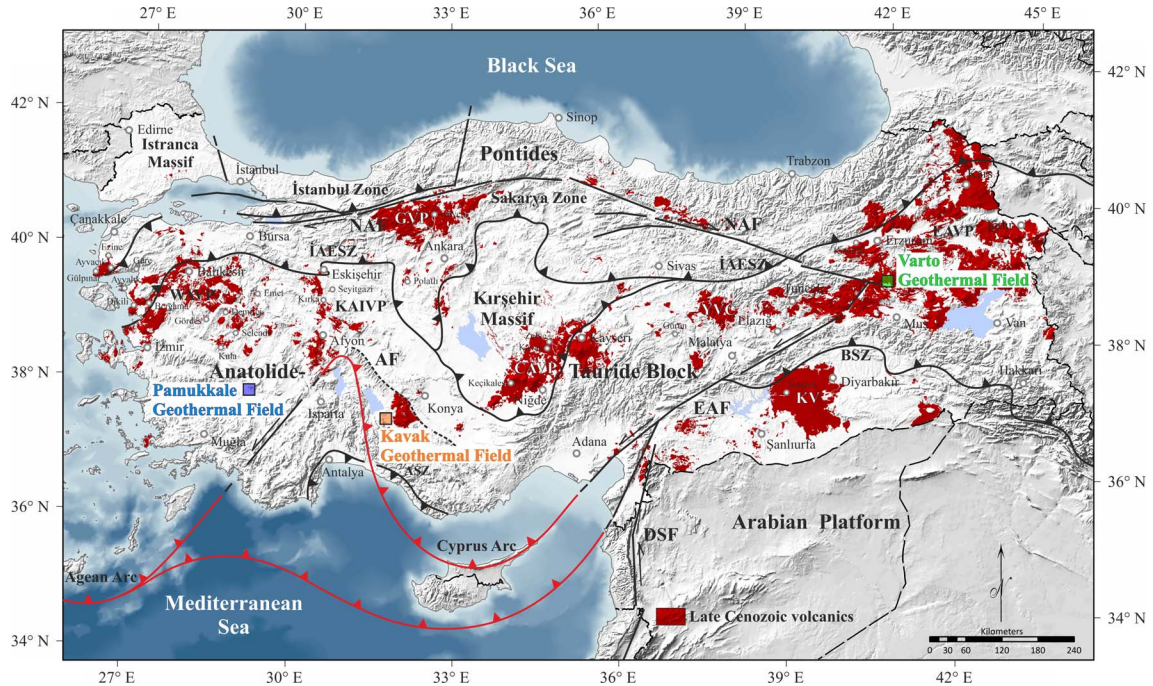


Figure 1. Simplified tectonic map of Turkey showing the major suture zones [Okay and Tüysüz, 1999], arc systems (red lines), continental blocks (black lines), and distribution of the main Post-Collision (Late Cenozoic) volcanic fields [MTA, 2013]. İAESZ: İzmir-Ankara-Erzincan Suture Zone, BSZ: Bitlis Suture Zone, ASZ: Antalya Suture Zone, NAF: North Anatolian Fault, EAF: East Anatolian Fault, DSF: Dead Sea Fault, AF: Afyon Fault, EAVP: East Anatolian volcanic provence, KV: Karacadağ volcanics, CAVP: central Anatolian volcanic provence, GVP: Galatian volcanic provence, ErAVC: Erenlerdağ-Alacadağ volcanic provence, KAIVP: Kirka-Afyon-Isparta volcanic provence, WAVP: West Anatolian volcanic provence.

their chemical compositions, surface temperatures and location.

The Central Tauride is an assemblage of various autochthonous and allochthonous crystalline-metamorphosed basement rocks [Dean and Monod, 1970, Göncüoğlu *et al.*, 2007, Göncüoğlu and Kozlu, 2000, Gürsu *et al.*, 2003, Moix *et al.*, 2008, Özgül, 1976, Robertson *et al.*, 2013, Şengör *et al.*, 2019, Turan, 2010]. The basement rocks around the KGF consist of Paleozoic metacarbonates and metaclastic rocks intercalated with metamarls [Karadağ, 2014]. These basement rocks are unconformably overlain by the Neogene-Quaternary sedimentary and volcanic rocks [Eren, 1996, Hakyemez *et al.*, 1992, Koç *et al.*, 2012, Özkan and Söğüt, 1998, Turan, 2020].

The Neogene volcanic rocks (ErAVC) cover approximately 1500 km² area (SW-Konya) and are separated from the Sulutas volcanic complex (SVC) by the Anatolide (Afyon zone) [Asan *et al.*, 2021] (Figure 2).

The ErAVC rocks are characterised by a large compositional range (53 wt% to 72 wt% SiO₂) and a unimodal distribution [Asan, 2017, Asan *et al.*, 2021] in the TAS diagram (Figure 4), and they were plotted into basaltic andesite represented by enclaves to rhyolite fields [Le Bas *et al.*, 1986]. The ErAVC rocks are calc-alkaline in the AFM diagram of Irvine and Baragar [1971], and have high-K content (Figures 5 and 6). These volcanic rocks were first described as calc-alkaline andesite and dacite, rarely basaltic andesite and rhyolitic composition, and they were suggested to be related to subduction-related magmatism by Keller *et al.* [1977]. The authors presented the first geological, geochemical (major oxides, very limited trace element, and Sr isotopes), and geochronological (K/Ar radiometric age) data of these rocks by Besang *et al.* [1977]. In these studies, it was shown that volcanic products are composed of lava domes/lava flow, pyroclastic fall and flow

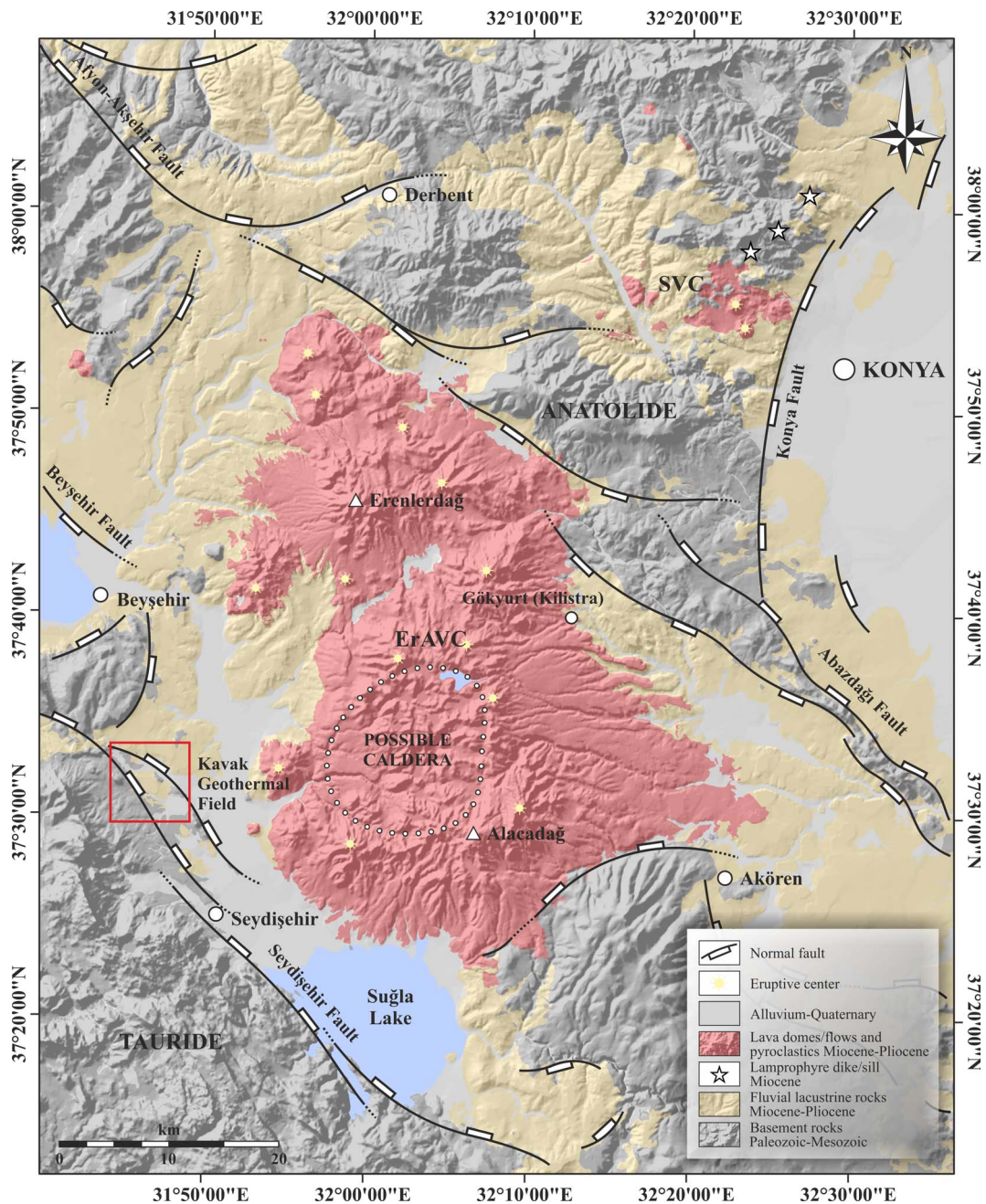


Figure 2. Simplified geological map of the west of Konya [Keller et al., 1977; General Directorate of Mineral Research and Explorations 1/100,000 geology map] from Gündüz [2023].

(e.g. block-and ash flows and ignimbrites) deposits [Keller et al., 1977]. It was stated by the researchers that the volcanism prolonged a wide period from Miocene (11.95 ± 0.02 Ma) to Pliocene (3.35 ± 0.08 Ma).

Sr–Nd isotopic data of the ErAVC presented by Temel et al. [1998] show that the intermediate and felsic volcanic rocks have high Sr and low Nd isotopes. The authors conclude that the rocks were related to the

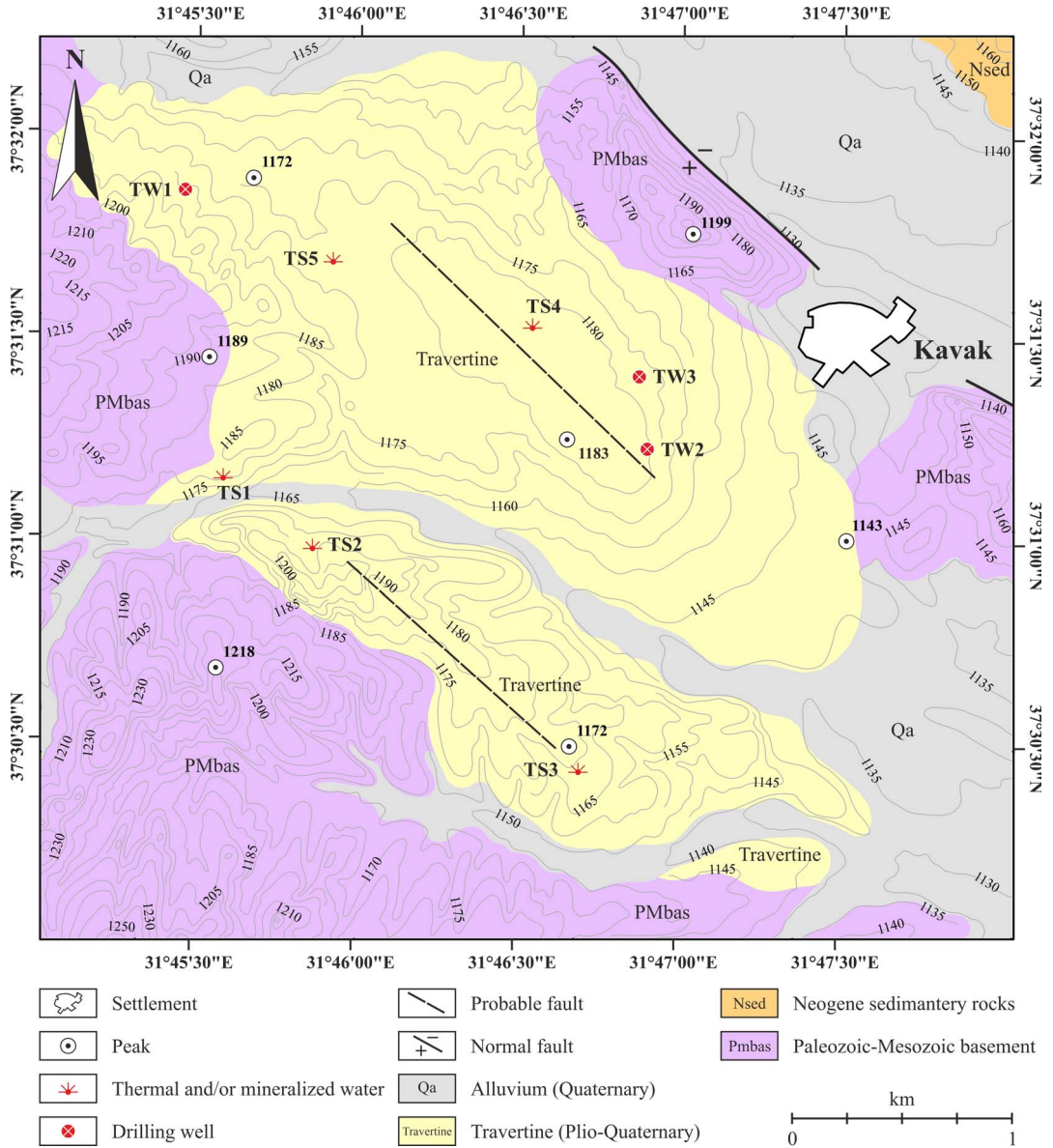


Figure 3. Geology map of the study area and location of thermal springs and drilling wells [Bozdağ, 2016].

subduction of the African plate under the Anatolian plate. On the other hand, Koçak and Zedef [2016] divided Konya volcanics into eight different lithological units and stated that these lithological units mainly contain mafic minerals (Mg# 0.69–0.71) (e.g. pyroxene “augite and enstatite”, calcic amphibole, biotite, opaques) and felsic minerals (e.g. plagioclase “An_{30–86}” and fewer quartz phenocryst) (Figure 7).

The Paleozoic metacarbonates that seem to be the main reservoir in the KGF have high permeability because of their highly fractured and karstified characteristics. Fractured quartzites of the Paleozoic metaclastic rocks are permeable whereas phyllite, clay, and metasiltstone within the Paleozoic metaclastics are relatively impermeable. Basin-filling limestones, conglomerates, and sandstones of the

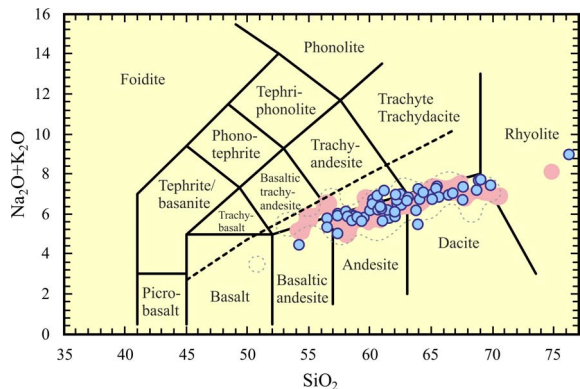


Figure 4. Geochemical classification diagrams of the ErAVC; pointed [Keller et al., 1977], gray dashed-line [Temel et al., 1998], pink-colored [Asan, 2017, Asan et al., 2023]: Total-Alkali Silica (TAS) diagram of [Le Bas et al., 1986]. Alkaline-sub alkaline division (dashed line) from Irvine and Baragar [1971]. All analyses were recalculated to 100% on a water-free basis for TAS classification.

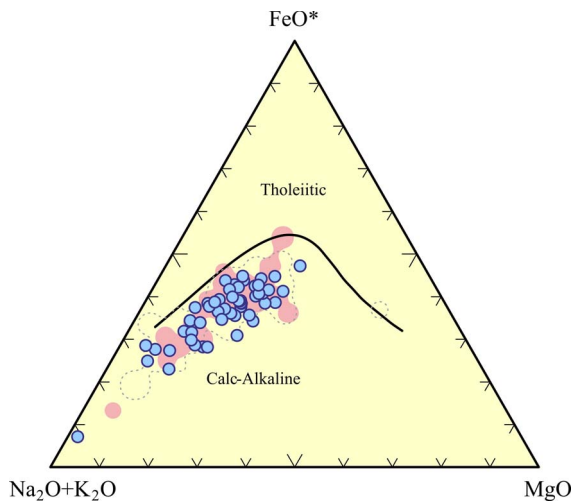


Figure 5. Sub-alkaline ErAVC rocks; pointed [Keller et al., 1977], gray dashed-line [Temel et al., 1998], pink-colored [Asan, 2017, Asan et al., 2023] on the AFM diagram [Irvine and Baragar, 1971].

Neogene-Quaternary sedimentary deposits are permeable, but silty and clayey layers are impermeable [Bozdağ, 2016]. Andesitic to rhyodacitic lavas from the ErAVC rocks acting as possible caprocks is impermeable whereas their pyroclastics (e.g. tuff, lapilli

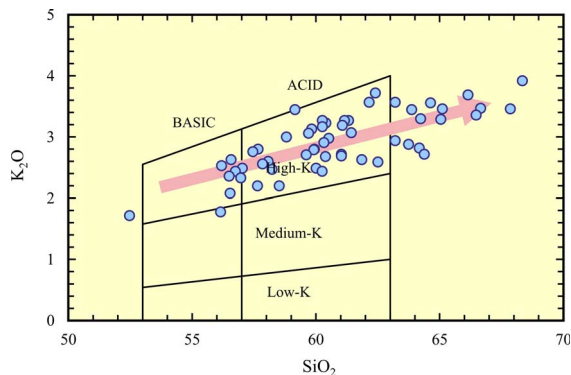


Figure 6. Plot of SiO₂ vs. K₂O (wt%) illustrating andesite types of Gill [1981]; pointed [Keller et al., 1977], pink-colored arrow [Asan, 2017, Asan et al., 2023].

tuff and breccia, etc.) are permeable. The ErAVC pyroclastics serving as possible geothermal reservoir or aquifer are widespread from the central to distal facies where they are interbedded with basin-filling fluvio-lacustrine deposits (Figures 2 and 3).

3. Material and methods

The published geochemical data from water and whole-rock samples in the KGF were used in this study. The water samples (e.g. thermal wells, springs, and cold waters) were analysed by Bozdağ [2016] for major anion-cation, trace elements, and isotope compositions in different geochemical laboratories (see the given reference for the detailed analytical methods of water samples). Metamorphic rock samples (e.g. metaclastics and metacarbonate) from the basement [Karadağ, 2014] and volcanic rock samples (e.g. lava flows, domes, enclaves and their pyroclastic equivalents) from the ErAVC [Asan, 2017, Asan et al., 2023, Karakaya, 2009, Keller et al., 1977, Temel et al., 1998] were analysed for major oxide and trace elements using XRF, ICP-OES or ICP-MS (see the given references for the detailed analytical methods of whole-rock samples).

In this study, cluster analysis and factor analysis were chosen as data analysis methods using GEOstats [Gündüz and Asan, 2022], a statistical data analysis program to perform these complex multivariate analyses. Using a class of cluster analysis designed to find groups of similar items within a data

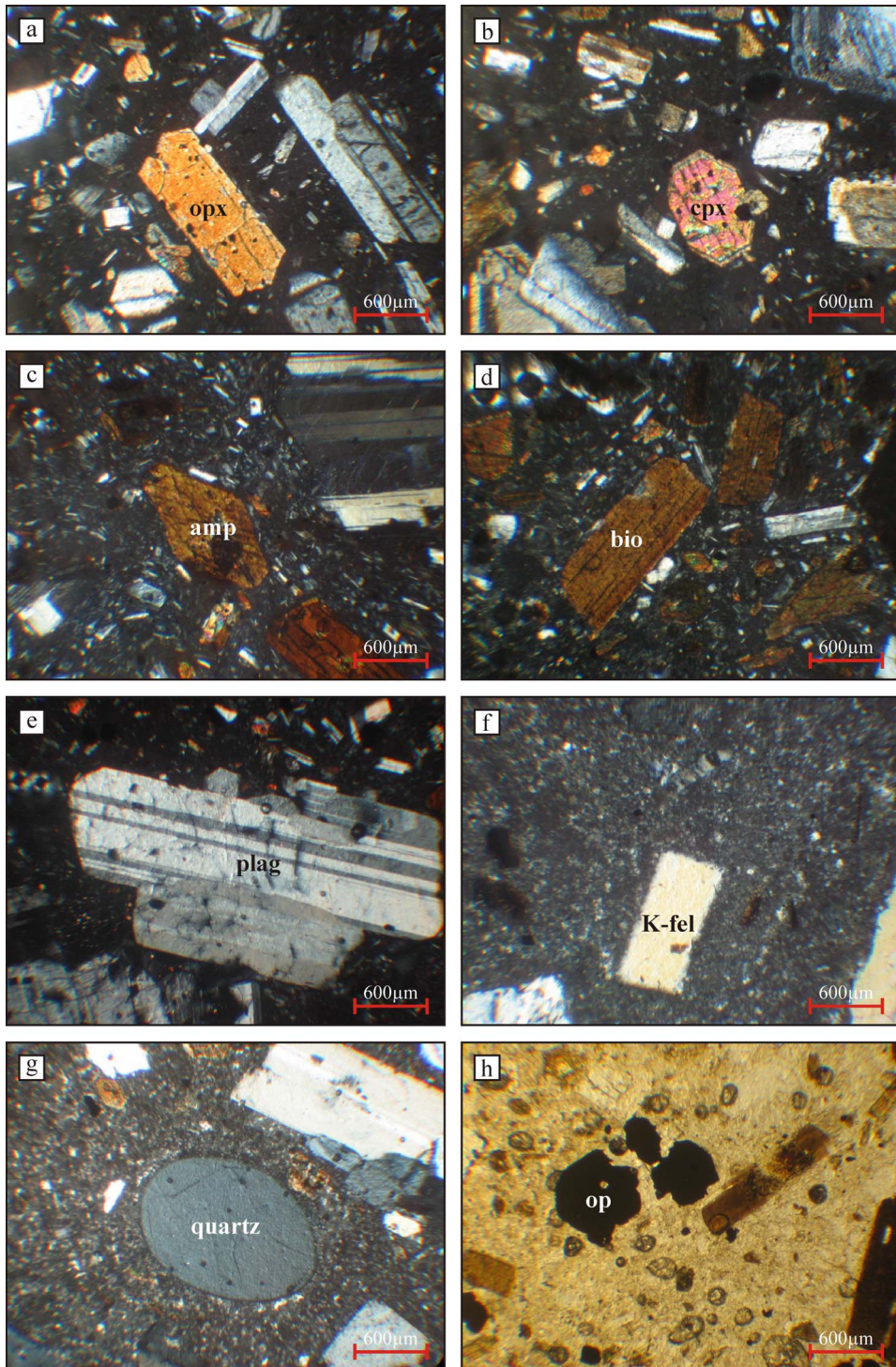


Figure 7. Microphotos of main mineralogical and textural features of the ErAVC rocks; (a) orthopyroxene, (b) clinopyroxene, (c) amphibole (hornblende), (d) biotite, (e) plagioclase, (f) K-feldspar (sanidine), (g) quartz and (h) opaque minerals (ilmenite or magnetite).

set, hierarchical cluster method produces a hierarchy of clusters, ranging from small clusters of very similar items to larger clusters of increasingly dissimilar items. The data matrix of cluster analysis is to be in standard form, $n \times p$ matrix with n rows of samples (e.g. sampling locations) and p columns of variables (e.g. geochemical data, discharge temperature, EC etc.). Computation may be in “Q-mode analysis (e.g. matrix size $n \times n$)” or “R-mode analysis (e.g. matrix size $p \times p$)”. R-mode analysis calculates distances (similarities) among all pairs of variables whereas Q-mode analysis calculates a matrix of distances between all pairs of samples. The hierarchical cluster analysis produces a graph known as a dendrogram. In dendrogram, the most similar two samples (e.g. A and B) are joined to form the first cluster, followed by another similar sample(s) (e.g. C or D) forming the second cluster, and so on. In this study, we first used “R-mode” to classify and characterise the KGF thermal waters based on the geochemical data, leading to the identification of homogeneous groups or subgroups in the data set. This grouping has the advantage to compare between water chemistry and rock or mineral chemistry, simplifying to interpret water-rock interactions. For example, if K, Na and Ba analysis results from thermal waters form a cluster, this can be interpreted to the interaction of thermal waters with a rock including alkali feldspar. On the other hand, Q-mode analysis was used to classify sampling locations into similar groups, and to identify thermal water types contributing to these groups. In this study, water samples taken along the KGF from 12 locations of which 4 locations are from cold waters and 8 locations from thermal waters (e.g. Cold Waters: CW1, CW2, CW3, CW4; Thermal Springs: TS1, TS2, TS3, TS4, TS5; Thermal Wells: TW1, TW2, TW3). These waters were evaluated by Q-mode analysis to identify water origins and tectonic (e.g. fault) control (e.g. spatial distribution) on their chemistry. For example, if springs are aligned along a lineament, sampling locations are to form a cluster in dendrogram as expected from fault-controlled springs. To test the grouping in the cluster analysis, we finally used factor analysis which is designed to reduce a large number of variables into fewer numbers of factors. Factor analysis collects variables into groups termed “factors”, which seem to behave similarly. Factor analysis is computed by “R-mode analysis” or “Q-mode analysis”. Therefore, it is anticipated that “factor analysis”

and “cluster analysis” produce similar groups as they do in this study.

4. Results

4.1. Hydrochemical characteristics of the Kavak thermal waters

In this study, the Piper diagram was used to assess the main chemical composition of the Kavak thermal waters. In addition, thermal water samples from the Pamukkale geothermal field [e.g. an example of interactions mainly with metamorphic rocks, Alçiçek *et al.*, 2019] and Varto geothermal field [e.g. an example of interactions mainly with volcanic rocks, Karaoğlu *et al.*, 2019] were selected to compare with the Kavak thermal waters (Figure 8).

The KGF can be characterised by two types of thermal waters based on the slight difference observed in their hydrochemistry. The first type thermal waters including TS1, TS2 and TS3 have higher TDS (up to 3200 mg/l) and Cl/Br ratio (950–1215), and lower dissolved silica (22–23 mg/l) and Br content (234–268 mg/l) relative to the second type water including TS4, TS5, TW1, TW2 and TW3 (TDS: 1850–2490 mg/l; Cl/Br ratio: 300–465; dissolved silica: 39–44 mg/l and Br content: 408–614 mg/l). Li, Cs, Rb, Mn, Fe, Cu, and As are also slightly higher, but Cl, Na, K, Ca, Mg, B, Ba, Sr and Zn concentrations are lower in second type thermal water than those of the first type. In addition, outlet temperatures of these thermal waters discharging along two different faults in north and south are also slightly different (e.g. ~ 22 °C for the first type of thermal waters and 25 to 46 °C for the second ones), and discharge along two different faults in north and south (see Figure 3).

Both type thermal waters in the KGF are chemically of Ca–Na–HCO₃ type although they show slight difference in their hydrochemistry. Also, they have higher total dissolved solids (TDS) values (average of 2566 mg/l) than those of cold waters (average of 359 mg/l) which probably offer long flow pathways, long residence times and intensive water–rock interactions [Bozdağ, 2016, Erbaş and Bozdağ, 2022]. Dissolution of the Paleozoic carbonates forming the main reservoir of thermal waters in the KGF is the reason for the high Ca²⁺ (283.1–549.4 mg/l) and HCO₃⁻ (1445–2687 mg/l) concentrations. Although the source of Mg²⁺ in Kavak thermal waters is mainly

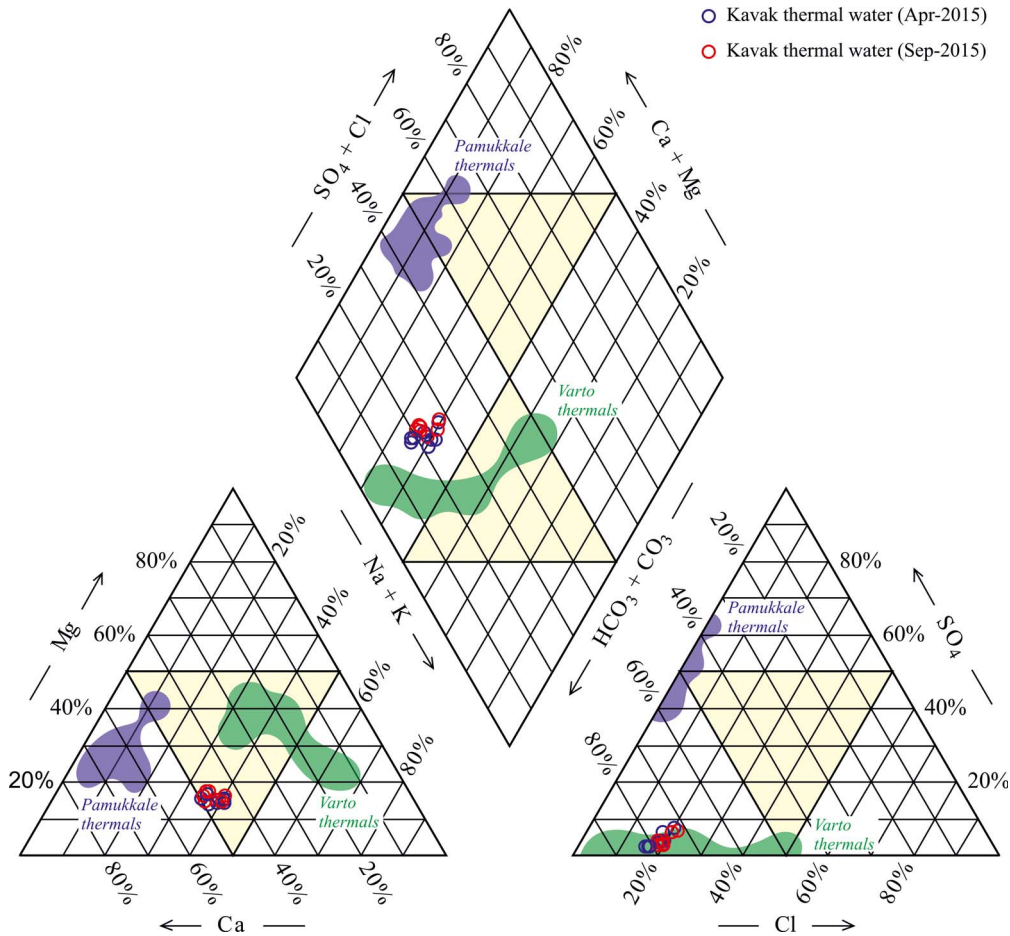


Figure 8. Piper plot showing the chemical composition of thermal waters in the Kavak geothermal field [Bozdağ, 2016]. Pamukkale thermals from Alçiçek et al. [2019] and Varto thermals from Karaoğlu et al. [2019].

the dissolution of dolomite and dolomitic limestone in the main aquifer in KGE, it is not the dominant cation. The reason for the low Mg values (average 72 mg/l) in thermal waters can be explained by the Mg depletion in the formation of phyllosilicates (e.g. clay minerals, chlorite and micas) in the Paleozoic metamorphics forming the secondary aquifer and/or ion exchange process. Na^+ (232–387 mg/l) is the second common cation in the thermal waters and K^+ (average 86 mg/l) is reached considerable values. Accordingly, the high Na^+ and K^+ in the Kavak thermal waters may be assumed to be derived from the decomposition mostly of intrusions of the ErAVC and regional metacrystalline rocks, progressive reactions with feldspar in the Paleozoic metamorphics and ion

exchange process. As also seen in the diagram, the similarity of the main ion concentrations of the Kavak thermal waters with that of the Varto thermal waters located in the south of the Varto caldera “alkaline and calc-alkaline volcanic rocks” [Buket and Temel, 1998] may be important for a better understanding of the relationship between regional geology and water-rock interaction.

The differences of major cations between Pamukkale and Varto thermal waters and the Kavak thermal waters can also be seen in the Schoeller diagram (Figure 9). The Kavak thermal waters have very high cation values compared to cold waters as a result of relatively deep and long-term circulation and contact with mainly volcanic rocks and partially

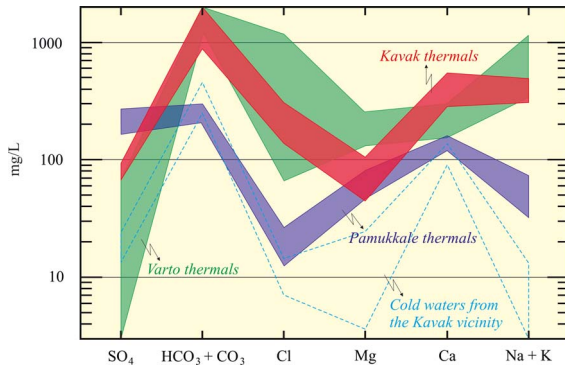


Figure 9. Semi-logarithmic Schoeller diagram, comparison of the concentrations of the Kavak geothermal (red line), the Pamukkale geothermal (darkblue line), and Varto (green line) samples. Pamukkale thermals from Alçiçek et al. [2019] and Varto themals from Karaoğlu et al. [2019].

crystalline basement or reservoir rocks. Additionally, Giggenbach's triangular diagram is often used for water classification in geochemical investigations performed in convergent-plate settings. In the diagram (Figure 10), the Kavak thermal water samples are located in the area of peripheral waters and this type water generally occurs at relatively shallow depths at some distance from the geothermal field.

It is known that silicate weathering is effective in terms of SiO_2 , Ca^{2+} , Mg^{2+} , Na^+ , and K^+ concentrations in groundwater. On the other hand, carbonate dissolution is effective in terms of Ca^{2+} , Mg^{2+} , and HCO_3^- concentrations. Accordingly, it is seen in the Ca/Na-Mg/Na diagram that the Kavak thermal waters fall close to the silicate weathering area and to the Varto thermal waters (Figure 11). The $(\text{Na}^+ + \text{K}^+) / (\text{Na}^+ + \text{K}^+ + \text{Ca}^{2+})$ ratios are higher than 0.45 indicating that the chemistry of the Kavak thermal waters is mainly controlled by the water-rock interaction. $(\text{Na}^+ + \text{K}^+ - \text{Cl}^-) / (\text{Na}^+ + \text{K}^+ - \text{Cl}^- + \text{Ca}^{2+})$ ratio < 0.20 , and $\text{Na}^+ / (\text{Na}^+ + \text{Cl}^-)$ ratio > 0.50 indicate that the source of Na^+ ion is plagioclase decomposition and ion exchange process [Hounslow, 1995]. Additionally, SiO_2 content, which is generally between 1–30 mg/l in natural waters, is higher than 30 mg/l in the Kavak thermal waters, indicating silicate weathering. The ion exchange process can be indicated by chloro-alkaline indices (CAI-1 and CAI-2) [Schoeller,

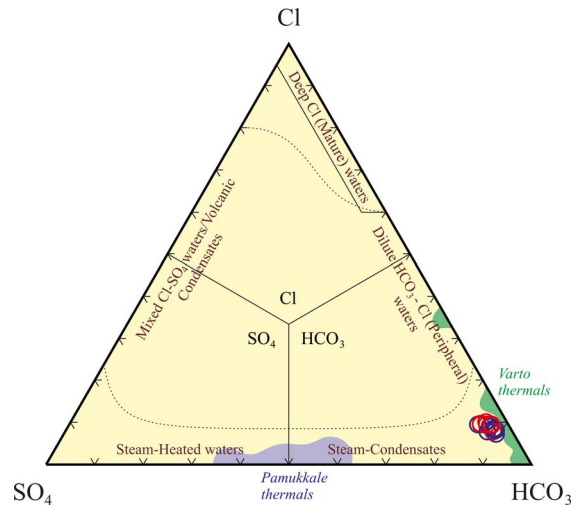


Figure 10. A triangular diagram of major anions has been suggested by Giggenbach [1988] for thermal waters, symbols as Figure 8. Pamukkale thermals from Alçiçek et al. [2019] and Varto themals from Karaoğlu et al. [2019].

1965], and negative CAI indices reflect the presence of ion exchange in the system. The CAIs are calculated by the following equations (all ionic concentrations are expressed by meq/L);

$$\text{CAI-1} = [\text{Cl}^- - (\text{Na}^+ + \text{K}^+)] / \text{Cl}^- \quad (1)$$

$$\text{CAI-2} = [\text{Cl}^- - (\text{Na}^+ + \text{K}^+)] / (\text{HCO}_3^- + \text{SO}_4^{2-} + \text{NO}_3^-). \quad (2)$$

The negative of CAI-1 and CAI-2 indicates that Ca^{2+} or Mg^{2+} ions in the groundwater have been replaced by Na^+ ion in a hydrodynamic medium (Figure 12). However, Şahinci [1991] specified that generally, the chloro-alkaline indices of water emerging from igneous and metamorphic rocks are also negative because the contribution of the alkali ions releasing from the decomposition of silicates is much more than the chloride ion. Accordingly, the hydrolysis of alkali feldspars in the Paleozoic metamorphics may be main process for especially high Na^+ ion in the Kavak thermal waters. However, the low Na_2O contents (< 1 wt%) and the low modal feldspar proportions of the Paleozoic metamorphites [Karadağ, 2014] indicate that neither ion exchange nor hydrolysis of alkali feldspars could not provide high sodium ions to thermal waters.

Table 1. R-mode correlation matrix of the Kavak thermal waters (for April 2015)

| | SiO ₂ | Ca | Mg | Na | K | Fe | Li | P | Rb | Sr | Ba | Al | Cs |
|------------------|------------------|-------|-------|-------|-------|-------|-------|-------|-------|-------|-------|-------|----|
| SiO ₂ | 1 | | | | | | | | | | | | |
| Ca | -0.86 | 1 | | | | | | | | | | | |
| Mg | -0.86 | 0.96 | 1 | | | | | | | | | | |
| Na | -0.76 | 0.96 | 0.98 | 1 | | | | | | | | | |
| K | -0.84 | 0.82 | 0.94 | 0.86 | 1 | | | | | | | | |
| Fe | 0.72 | -0.28 | -0.31 | -0.11 | -0.44 | 1 | | | | | | | |
| Li | 0.79 | -0.67 | -0.59 | -0.47 | -0.56 | 0.72 | 1 | | | | | | |
| P | -0.62 | 0.74 | 0.78 | 0.81 | 0.79 | -0.07 | -0.26 | 1 | | | | | |
| Rb | 0.70 | -0.48 | -0.43 | -0.29 | -0.47 | 0.78 | 0.95 | -0.18 | 1 | | | | |
| Sr | -0.94 | 0.92 | 0.96 | 0.90 | 0.94 | -0.48 | -0.63 | 0.84 | -0.52 | 1 | | | |
| Ba | -0.96 | 0.93 | 0.95 | 0.89 | 0.90 | -0.50 | -0.67 | 0.79 | -0.55 | 0.99 | 1 | | |
| Al | 0.12 | -0.18 | -0.09 | -0.16 | 0.12 | -0.12 | -0.25 | -0.01 | -0.36 | -0.08 | -0.14 | 1 | |
| Cs | 0.40 | -0.19 | -0.08 | 0.05 | -0.06 | 0.69 | 0.81 | 0.34 | 0.80 | -0.12 | -0.17 | -0.23 | 1 |

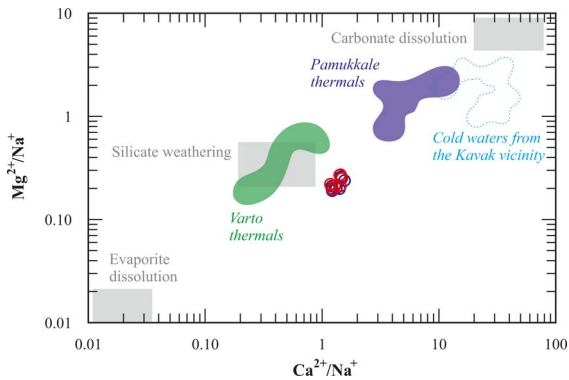


Figure 11. $\text{Ca}^{2+}/\text{Na}^{+}$ vs. $\text{Mg}^{2+}/\text{Na}^{+}$ diagram showing end-members; Evaporite dissolution, Silicate weathering, and Carbonate dissolution, symbols as Figure 8. Pamukkale thermals from Alçiçek et al. [2019] and Varto themals from Karaoğlu et al. [2019].

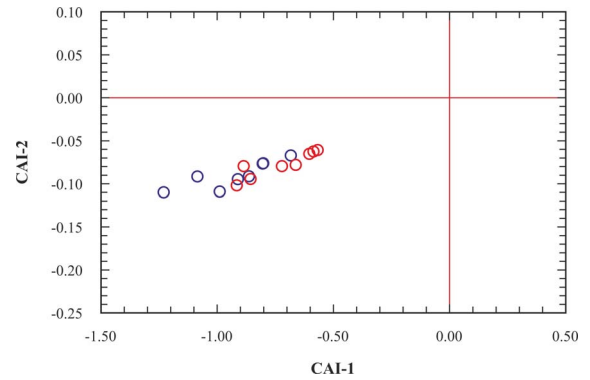


Figure 12. Chloro-alkaline indices (CAI) of the Kavak geothermal waters, symbols as Figure 8.

4.2. Data analysis and geochemical origin of the Kavak thermal waters

To better understand the details of the water–rock interaction and to classify sampling locations into similar groups, and to identify two types of thermal water contributing to these groups in the KGF, data analysis methods were performed by using the published hydrochemistry data from Bozdağ [2016]. Firstly, cluster analysis was performed by the method

of shortest distance on the Kavak thermal waters to reveal the relationship between thermal water and rocks/minerals based on the R-mode analysis and to research spatial distribution of two types of thermal waters (e.g. their relationship with the faults) based on the Q-mode analysis. The clustering analysis and factor weights were calculated for variables from thermal water taken from 8 different locations (TS1, TS2, TS3, TS4, TS5; TW1, TW2, TW3) in the Kavak geothermal field by using GEOstats [Gündüz and Asan, 2022].

The hierarchical cluster analysis with R-mode is based on correlation coefficients (Table 1), producing dendrogram (Figure 13). The dendrogram con-

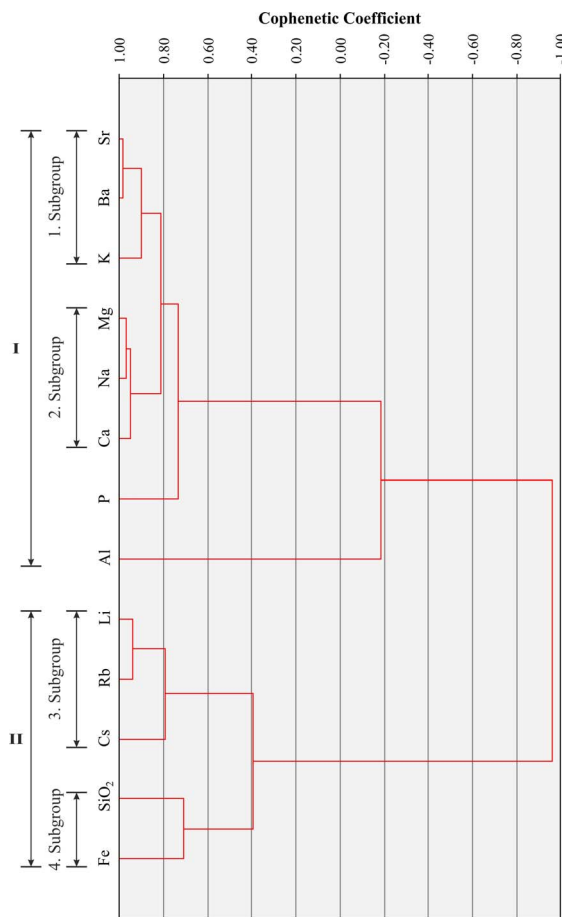


Figure 13. R-mode cluster analysis (Dendrogram) of the Kavak thermal waters (single-linkage method).

sists of two main groups (Group I: K, Ba, Sr, Ca, Na, Mg, Al, P; Group II: Cs, Rb, Li, Fe, SiO₂) and 4 sub-groups. These groups may be attributed to rock-forming minerals especially in volcanic rocks represented by the ErAVC and metamorphic rocks from the basement. For example, Subgroup (1) Sr, Ba and K are important components for biotite and K-feldspar: sanidine is modally rare in the ErAVC rocks, but they have high normative orthoclase (Or; KAlSi₃O₈ end-member) content (Table 2). K may also be associated with sericite, and other phyllosilicate minerals in the crystalline basement rocks (e.g. phyllite, schist, etc.). On the other hand, Sr is an important element for plagioclases as a result of Ca-Sr substitution. Subgroup (2) Na, Ca and Mg may be interpreted to plagioclase and mafic silicates (e.g. amphibole, pyrox-

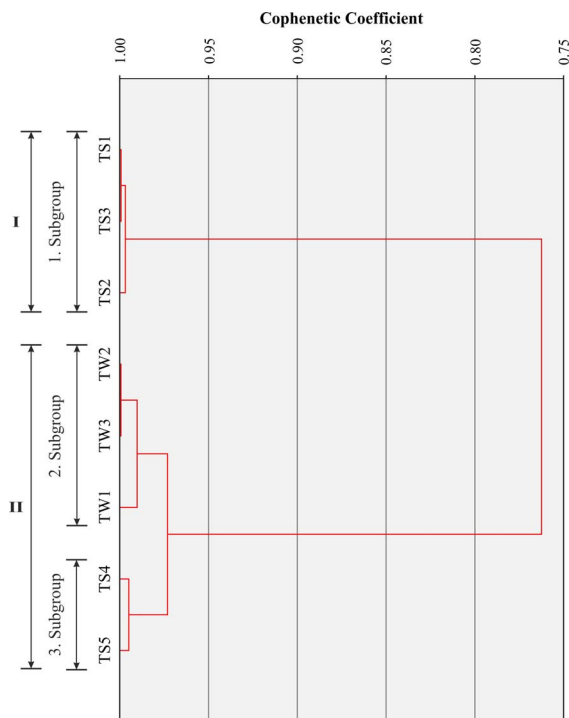


Figure 14. Q-mode cluster analysis (Dendrogram) of the Kavak thermal waters (single-linkage method).

Table 2. Results of CIPW norm calculation (%) of the ErAVC [Asan, 2017, Asan et al., 2023]

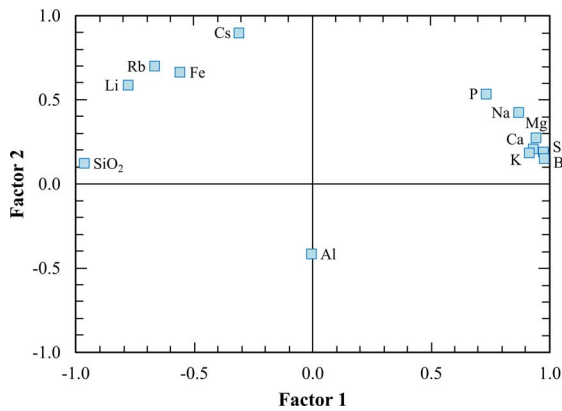
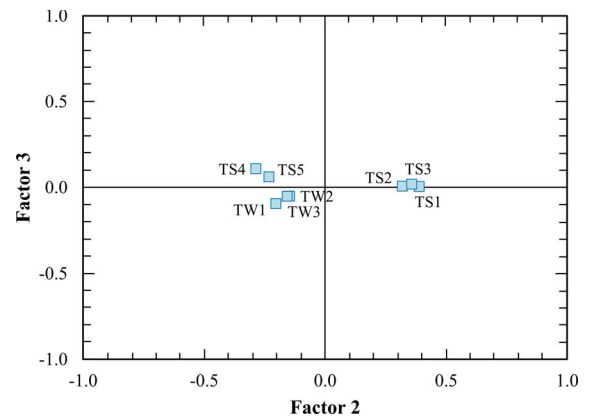
| | Min | Max | Mean |
|------------|-------|-------|-------|
| Quartz | 0.99 | 27.75 | 13.27 |
| Anorthite | 13.02 | 28.52 | 21.21 |
| Albite | 20.90 | 34.19 | 27.80 |
| Orthoclase | 9.87 | 24.29 | 18.26 |
| Pyroxene | 6.88 | 30.43 | 16.24 |
| Ilmenite | 0.63 | 1.98 | 1.29 |
| Magnetite | 0.64 | 2.45 | 1.31 |

ene) in volcanic rocks or calcite-dolomite in meta-carbonate rocks. Also, Al and P can be accepted in the same group as plagioclase and apatite minerals, respectively. Subgroups (3) and (4) Li, Rb, Cs, Fe, and Si are important in the crystal structure of amphiboles and biotites.

The Cluster analysis based on the Q-mode forms two main groups (Group I: TS1, TS2, TS3; Group II:

Table 3. Q-mode correlation matrix of the Kavak thermal waters (for April 2015)

| | TS1 | TS2 | TS3 | TS4 | TS5 | TW1 | TW2 | TW3 |
|-----|-------|-------|-------|-------|-------|-------|-------|-----|
| TS1 | 1 | | | | | | | |
| TS2 | 0.997 | 1 | | | | | | |
| TS3 | 0.999 | 0.999 | 1 | | | | | |
| TS4 | 0.763 | 0.808 | 0.785 | 1 | | | | |
| TS5 | 0.801 | 0.844 | 0.822 | 0.995 | 1 | | | |
| TW1 | 0.813 | 0.855 | 0.830 | 0.973 | 0.986 | 1 | | |
| TW2 | 0.849 | 0.884 | 0.865 | 0.975 | 0.987 | 0.990 | 1 | |
| TW3 | 0.845 | 0.881 | 0.861 | 0.977 | 0.989 | 0.993 | 0.999 | 1 |

**Figure 15.** R-mode factor weights of the Kavak thermal waters on the diagram.**Figure 16.** Q-mode factor weights of the Kavak thermal waters on the diagram.

TW1, TW2, TW3, TS4, TS5) and three subgroups (Figure 14, Table 3). The Group I, including subgroup 1, is represented by the first type of thermal waters (e.g. higher TDS and Cl/Br ratio, and lower dissolved silica and Br content with discharge temperature of 22 °C) discharged along the southern fault whereas the Group II includes the second type thermal waters (e.g. lower TDS and Cl/Br ratio, and higher dissolved silica and Br content with discharge temperature of 25 to 46 °C) discharged along the northern fault, which is close to the ErAVC (see Figures 2, 3). In the Group II, well samples (e.g. Subgroup 2; TW1, TW2, TW3) and spring samples (e.g. Subgroup 3; TS4, TS5) also form two separate subgroups.

The grouping of elements resulted from R-mode and Q-mode factor analysis is similar to hierarchical clustering analysis. In R-mode factor analysis

(Figure 15, Table 4), K, Sr, Ba, Ca, Na, Mg and P form a group similar to those of the Group I in the R-mode cluster analysis, whereas SiO₂, Li, Rb, Fe and Cs form another group similar to the Group II in the R-mode cluster analysis. On the other hand, in Q-mode factor analysis (Figure 16, Table 5), TS1, TS2, TS3 samples from the first type thermal waters and TW1, TW2, TW3, TS4, TS5 samples from the second type thermal waters form two separate groups as in Q-mode cluster analysis.

5. Water-rock interaction and conceptual model of the Kavak geothermal field

Whole rock- and mineral chemistry of volcanic rocks are key features of better understanding the water-rock interaction in geothermal fields such as KGF where volcanic rocks act as a heat source. The relative

Table 4. R-mode factor analysis and eigenvalue results of the Kavak thermal waters for 13 variables

| Component | Factor 1 | Factor 2 | Factor 3 | Factor 4 | Factor 5 |
|----------------------------|----------|----------|----------|----------|----------|
| SiO ₂ | -0.965 | 0.116 | 0.181 | 0.146 | 0.006 |
| Ca | 0.934 | 0.202 | -0.107 | 0.270 | -0.037 |
| Mg | 0.946 | 0.268 | 0.025 | 0.109 | 0.142 |
| Na | 0.872 | 0.420 | 0.017 | 0.234 | 0.090 |
| K | 0.917 | 0.177 | 0.223 | -0.149 | 0.219 |
| Fe | -0.561 | 0.661 | 0.168 | 0.464 | -0.064 |
| Li | -0.780 | 0.583 | -0.006 | -0.205 | 0.089 |
| P | 0.735 | 0.529 | 0.262 | -0.147 | -0.287 |
| Rb | -0.668 | 0.697 | -0.093 | -0.041 | 0.165 |
| Sr | 0.977 | 0.183 | 0.009 | -0.105 | -0.004 |
| Ba | 0.980 | 0.144 | -0.083 | -0.073 | -0.032 |
| Al | -0.004 | -0.427 | 0.900 | 0.025 | 0.056 |
| Cs | -0.311 | 0.896 | 0.180 | -0.237 | -0.058 |
| Eigenvalue | 8.22 | 2.92 | 1.05 | 0.54 | 0.21 |
| Cumulative eigenvalue | 8.22 | 11.13 | 12.18 | 12.72 | 12.93 |
| Variability (%) | 63.22 | 22.43 | 8.08 | 4.13 | 1.59 |
| Cumulative variability (%) | 63.22 | 85.65 | 93.73 | 97.85 | 99.45 |

Table 5. Q-mode factor analysis and eigenvalue results of the Kavak thermal waters for 8 variables

| Component | Factor 1 | Factor 2 | Factor 3 | Factor 4 | Factor 5 |
|----------------------------|----------|----------|----------|----------|----------|
| TS1 | 0.920 | 0.392 | 0.004 | -0.004 | -0.001 |
| TS2 | 0.947 | 0.322 | 0.007 | 0.020 | 0.004 |
| TS3 | 0.933 | 0.360 | 0.019 | -0.004 | -0.001 |
| TS4 | 0.951 | -0.288 | 0.110 | -0.004 | 0.021 |
| TS5 | 0.970 | -0.233 | 0.061 | 0.026 | -0.027 |
| TW1 | 0.972 | -0.205 | -0.096 | 0.059 | 0.009 |
| TW2 | 0.986 | -0.148 | -0.049 | -0.056 | -0.002 |
| TW3 | 0.985 | -0.158 | -0.051 | -0.035 | -0.002 |
| Eigenvalue | 7.35 | 0.61 | 0.03 | 0.01 | 0.01 |
| Cumulative eigenvalue | 7.35 | 7.96 | 7.99 | 8.00 | 8.00 |
| Variability (%) | 91.82 | 7.67 | 0.38 | 0.11 | 0.02 |
| Cumulative variability (%) | 91.82 | 99.49 | 99.87 | 99.98 | 100.00 |

cation chemistry of waters is compared with rocks in Ca–Mg–Na+K triangular plot to research water–rock interaction in the KGF. In the Ca–Mg–Na+K triangular diagram, both the ErAVC volcanic rocks and the Kavak thermal waters plotting close to the Na+K field

suggest that high Na–K concentrations of the Kavak thermal waters can be related to the ErAVC volcanic rocks and their intrusions. However, the cold waters show a high tendency towards Ca and Ca+Mg around the KGF (Figures 17 and 18).

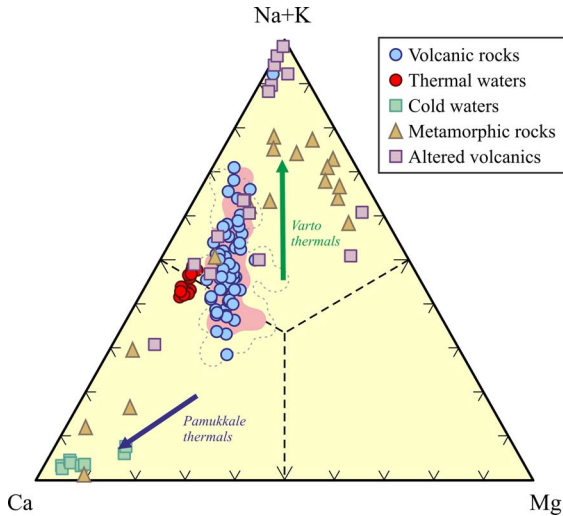


Figure 17. The relative cation chemistry of the Kavak thermal and cold water [Bozdağ, 2016] and comparison with the Er-AVC rocks; pointed [Keller *et al.*, 1977], gray dashed-line [Temel *et al.*, 1998], pink-colored [Asan, 2017, Asan *et al.*, 2023] in the (Na+K)–Ca–Mg triangular plot. Altered volcanics are from Karakaya [2009]. Metamorphic rocks (metapelites, metapsammities, and metamarls) are from Karadağ [2014].

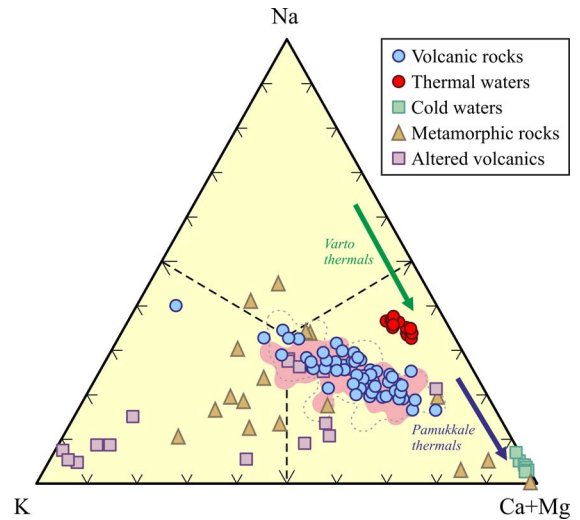


Figure 18. The relative cation chemistry of the Kavak thermal water and cold water [Bozdağ, 2016] and comparison with the Er-AVC rocks; pointed [Keller *et al.*, 1977], gray dashed-line [Temel *et al.*, 1998], pink-colored [Asan, 2017, Asan *et al.*, 2023] in the Na–K–(Ca+Mg) triangular plot. Altered volcanics are from Karakaya [2009]. Metamorphic rocks (metapelites, metapsammities, and metamarls) are from Karadağ [2014].

The Kavak geothermal field is recharged mainly by infiltrating of meteoric waters, which go down through the faults and fracture/cracks systems acting as hydrothermal conduits [Bozdağ, 2016]. The infiltrated waters are heated by the high thermal gradient of the Neogene (Miocene–Pliocene) Erenlerdağ–Alacadağ volcanic rocks in the deep, and then the density of these waters heated at the deep decreases as a result of increasing temperature and pressure, and so the thermal waters move up to the surface and/or shallower depths of the hydrothermal pathways (Figure 19). The low tritium values [<1 TU; Bozdağ, 2016] of the Kavak thermal waters also suggest deep circulation and longer residence times. The following geological model of the region (Figure 19) is also supported by the $\delta^{13}\text{C}$ values in the Kavak travertines and thermal waters because high $\delta^{13}\text{C}$ is revealed as a result of reaching very deep the faults fractures in the region [Karaisoğlu and Orhan, 2018].

Fractured and karstified Palaeozoic carbonates constitute the main reservoir rocks for the Kavak

geothermal waters and, pyroclastic rocks of the Er-AVC can be accepted as the secondary aquifer. Fine-grained metasandstone, metasiltstone and phyllite in the Paleozoic metamorphites and the clayey and silty levels of the Neogene units act as cap rocks for the Kavak geothermal system. The chemical composition of the Kavak thermal waters is mainly controlled water–rock interactions including dissolution of the Paleozoic carbonates, and the decomposition mostly of intrusions of the ErAVC.

Based on the chemical and statistical data, it has been identified that there are two distinct types of the thermal waters in the KGF. The reason for the occurrence of two different types of thermal waters is thought to be that the fault in the south, where the first type of thermal waters (TS1, TS2 and TS3) are located, acts as a barrier or semi-barrier. This is because faults act as a barrier and/or channel for flow, depending on their composition and the stage of fault evolution. In other words, a fault may act as a conduit immediately after deformation and it can

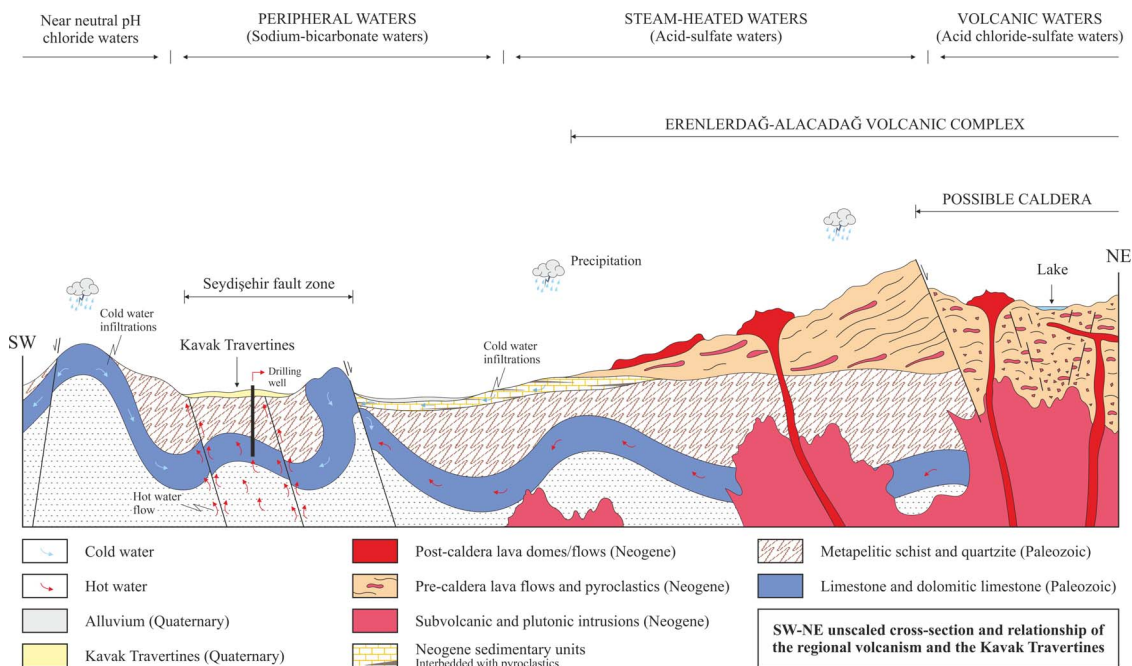


Figure 19. Unscaled schematic illustration of the Erenlerdağ–Alacadağ volcanic complex (ErAVC) and Kavak Travertines modified from Bozdağ [2016]. The geochemical framework of the geothermal systems that are related to subduction zone volcanism [Henley and Ellis, 1983].

later act as a barrier due to the precipitation of minerals [Caine *et al.*, 1996]. Therefore, the partial interruption of the relationship between the first and second types of the thermal waters due to the southern fault resulted in slight differences, particularly in the minor ion contents and TDS values. In addition, the mixing of the first type of thermal water with colder water caused a greater decrease in temperature compared to the second type of thermal water.

6. Conclusions

In this study, the water–rock interaction mechanism was investigated based on the multivariate statistical analysis (e.g. factor analysis and clustering analysis) using the published water and whole rock geochemical data from the Kavak Geothermal Field (Konya, Turkey). The Kavak Geothermal Field (KGF) is controlled by the Seydişehir fault that is a part of a graben-like structure in an extensional basin. The KGF overlies a metamorphic basement, yet is located near the Erenlerdağ–Alacadağ volcanic complex (ErAVC). The metamorphic basement is

represented by low-degree metaclastic and metacarbonate rocks whereas the volcanic rocks are composed of orogenic-type high-K calc-alkaline andesite and rhyodacite. The Kavak thermal waters are meteoric in origin and peripheral waters (Ca–Na–HCO₃), and are characterised by high K⁺ and Na⁺ cations, and low pH (between 6.4–6.9 pH) values relative to the cold waters. Two types of thermal waters were identified in the KGF based on the slight difference in their hydrochemistry. The first type thermal water has higher TDS and Cl/Br ratio, and lower dissolved silica and Br content relative to the second type water. These thermal waters lying along two different faults also have a slightly different discharge temperature. Q-mode cluster and factor analysis confirmed that first type and second type thermal waters formed two separate statistical groups, which is compatible with the observed slight geochemical differences between two types of thermal waters. The reason for the occurrence of two different types of thermal waters is thought to be that the fault in the south, where the first type of thermal waters (TS1, TS2 and TS3) are located, acts as a barrier or semi-barrier.

Mixing of the first type of thermal water with colder water also caused a greater decrease in temperature compared to the second type of thermal water.

When compared, hydrochemical properties of the Kavak thermal waters are similar to the ErAVC relative to the metamorphic basement rocks. R-mode cluster and factor analysis performed in this study suggests that the chemistry of the KGF waters was mainly controlled by the composition of the ErAVC rather than those of the basement metamorphic rocks as a result of water–rock interaction based on the quantitative of cation exchanges. In this regard, the Kavak geothermal system was revised to a new conceptual model considering the influence of the heat source on the chemistry of the regional thermal waters as a result of water–rock interaction.

Declaration of interests

The authors do not work for, advise, own shares in, or receive funds from any organization that could benefit from this article, and have declared no affiliations other than their research organizations.

Acknowledgments

This article is based on the first author's study at University of Poitiers. The authors thank to the editor Dr. François Chabaux and an anonymous reviewer for their critical and constructive comments that improved the quality of this paper. The first author also thanks to Campus France for scholarships to foreign students in France.

References

- Aksoy, R. (2019). Extensional neotectonic regime in West–Southwest Konya. Central Anatolia, Turkey. *Int. Geol. Rev.*, 61(14), 1803–1821.
- Alçiçek, H., Bülbül, A., Yavuzer, I., and Alçiçek, M. C. (2019). Origin and evolution of the thermal waters from the Pamukkale Geothermal Field (Denizli Basin, SW Anatolia, Turkey): insights from hydrogeochemistry and geothermometry. *J. Volcanol. Geotherm. Res.*, 372, 48–70.
- Asan, K. (2017). *Çarpışma Sonrası Ortamda Ultrapotasikten Kalk-alkalen Volkanizmaya Geçişin Jeokimyasal ve Sr–Nd–Pb İzotopik Özellikleri, Konya–Türkiye*. Tübitak, Konya. Proje No: 113Y415.
- Asan, K., Kurt, H., Gündüz, M., and Gençoğlu Korkmaz, G. (2023). Geochemistry and Petrology of the Unimodal Versus Bimodal Neogene Volcanism in the Konya Volcanic Field. Central Anatolia, Turkey. (under review).
- Asan, K., Kurt, H., Gündüz, M., Gençoğlu Korkmaz, G., and Ganerød, M. (2021). Geology, geochronology and geochemistry of the miocene sulutas volcanic complex, Konya-Central Anatolia: genesis of orogenic and anorogenic rock associations in an extensional geodynamic setting. *Int. Geol. Rev.*, 63(2), 161–192.
- Bayram, A. F. (1992). *Seydişehir ve Kaşaklı sıcaksu kaynaklarının hidrojeoloji incelenmesi*. Selçuk University, Konya.
- Besang, C., Eckhardt, F. J., Harre, W., Kreuzer, H., and Müller, P. (1977). Radiometrische Altersbestimmungen an neogenen Eruptivgesteinen der Türkei. *Geol. Jahrb.*, B25, 3–36.
- Bozdağ, A. (2016). Hydrogeochemical and isotopic characteristics of Kavak (Seydişehir-Konya) geothermal field, Turkey. *J. Afr. Earth Sci.*, 121, 72–83.
- Buket, E. and Temel, A. (1998). Major-element, trace-element, and Sr–Nd isotopic geochemistry and genesis of Varto (Muş) volcanic rocks, Eastern Turkey. *J. Volcanol. Geotherm. Res.*, 85(1–4), 405–422.
- Burçak, M., Duman, O., and Bekar, K. (2002). *Seydişehir (Konya)-Kavakköy Jeotermal Sahası Jeotermal-Jeofizik Etüt Raporu*. Raport No: 10666. General Directorate of Mineral Research and Exploration (MTA), Ankara.
- Caine, J. S., Evans, J. P., and Forster, C. B. (1996). Fault zone architecture and permeability structure. *Geol. Soc. Am.*, 24, 1025–1028.
- Davraz, A., Nalbantçılar, M. T., and Önden, İ. (2022a). Hydrogeochemical characteristics and trace element of geothermal systems in Central Anatolia, Turkey. *J. Afr. Earth Sci.*, 195, article no. 104666.
- Davraz, A., Nalbantçılar, M. T., Varol, S., and Önden, İ. (2022b). Hydrogeochemistry and reservoir characterization of the Konya geothermal fields, Central Anatolia/Turkey. *Geochem. Geophys. Geosyst.*, 82(2), article no. 125867.
- Dean, W. T. and Monod, O. (1970). The Lower Paleozoic stratigraphy and faunas of the Taurus Mountains near Beyşehir, Turkey. I. Stratigraphy. *Bull. Br. Mus. (Nat. Hist.) Geol.*, 19, 411–426.

- Erbaş, H. A. and Bozdağ, A. (2022). Hydrogeochemical characteristics and evaluation of the geothermal fluids in the Gazlıgöl geothermal field (Afyonkarahisar), Western Anatolia, Turkey. *Geothermics*, 105, article no. 102543.
- Eren, Y. (1996). Sille-Tatköy (Bozdağlar masifi-Konya) kuzeyinde Alpin öncesi bindirmeler. *Türkiye Jeoloji Kurultayı Bülteni*, 11, 163–169.
- Giggenbach, W. F. (1988). Geothermal solute equilibria. Derivation of Na–K–Ca–Mg geothermometers. *Geochim. Cosmochim. Acta*, 52(12), 2749–2765.
- Gill, J. B. (1981). In *Orogenic Andesites and Plate Tectonics*, page 401. Springer Verlag, Berlin.
- Göçmez, G., Kara, İ., Nalbantçılar, M. T., and Güzel, A. (2005). In *Konya'daki Sıcak ve Mineralli suların Hidrokimyasal Özellikleri, II*, pages 121–132. Ulusal Hidrolojide İzotop Teknikleri Sempozyumu, İzmir.
- Göçmez, G. and Şen, O. (1998). Kavakköy Seydişehir çevresinin jeoloji ve hidrojeoloji incelemesi. In *F.Ü. Jeoloji eğitiminin 20. yıl sempozyum bildirileri, Elazığ*, pages 607–613.
- Göncüoğlu, M. C., Çapkınoğlu, Ş., Gürsu, Ş., Noble, P., Turhan, N., Tekin, U. K., Okuyucu, C., and Göncüoğlu, Y. (2007). The Mississippian in the Central and Eastern Taurides (Turkey): constraints on the tectonic setting of the Tauride-Anatolide Platform. *Geol. Carpathica*, 58(5), 427–442.
- Göncüoğlu, M. C. and Kozlu, H. (2000). Early Paleozoic evolution of the NW Gondwanaland: data from southern Turkey and surrounding regions. *Gondwana Res.*, 3(3), 315–323.
- Gündüz, M. (2023). *The origin and eruption mechanism of the Kilistra ignimbrites deduced from chemostratigraphic, geochronologic, remote sensing, and GIS methods, Erenlerdağ-Alacadağ volcanic complex SW Konya-Central Anatolia*. Phd thesis, Muğla Sıtkı Koçman University, Muğla. 194.
- Gündüz, M. and Asan, K. (2022). GEOstats: an excel-based data analysis program applying basic principles of statistics for geological studies. *Earth Sci. Inf.*, 15, 705–712.
- Gürsu, S., Kozlu, H., Göncüoğlu, M. C., and Turhan, N. (2003). Orta Torosların Batı Kesimindeki Temel Kayaları ve Alt Paleozoyik Örtülerinin Korelasyonu. *TPJD Bülteni*, C.15(s.2), 129–153.
- Hakyemez, Y., Elibol, E., Umut, M., Bakırhan, B., Kara, İ., Dağistan, H., Metin, T., and Erdoğan, N. (1992). Konya-Çumra-Akören dolayının jeolojisi. Rapor No: 9449, MTA Ankara.
- Hao, C., Huang, Y., Ma, D., and Fan, X. (2020). Hydro-geochemistry evolution in Ordovician limestone water induced by mountainous coal mining: A case study from North China. *J. Mt. Sci.*, 17, 614–623.
- Henley, R. W. and Ellis, A. J. (1983). Geothermal systems ancient and modern: a geochemical review. *Earth-Sci. Rev.*, 19(1), 1–50.
- Hounslow, A. W. (1995). In *Water Quality Data: Analysis and Interpretation*, page 416. CRC Press, Boca Raton.
- Irvine, T. N. and Baragar, W. R. A. (1971). A guide to the chemical classification of the common volcanic rocks. *Can. J. Earth Sci.*, 8(5), 523–548.
- Karadağ, M. M. (2014). Geochemistry, provenance and tectonic setting of the Late Cambrian-Early Ordovician Seydişehir Formation in the Çaltepe and Fele areas, SE Turkey. *Geochemistry*, 74(2), 205–224.
- Karaisaoğlu, S. and Orhan, H. (2018). Sedimentology and geochemistry of the Kavakköy Travertine (Konya, central Turkey). *Carbonates Evaporites*, 33, 783–800.
- Karakaya, N. (2009). REE and HFS element behaviour in the alteration facies of the Erenler Dağı Volcanics (Konya, Turkey) and kaolinite occurrence. *J. Geochem. Explor.*, 101(2), 185–208.
- Karaoğlu, Ö., Bazargan, M., Baba, A., and Browning, J. (2019). Thermal fluid circulation around the Karliova triple junction: Geochemical features and volcano-tectonic implications (Eastern Turkey). *Geothermics*, 81, 168–184.
- Keegan-Treloar, R., Irvine, D. J., Solorzano-Rivas, S. C., Werner, A. D., Banks, E. W., and Currell, M. J. (2022). Fault-controlled springs: A review. *Earth-Sci. Rev.*, 230, article no. 104058.
- Keller, J., Jung, D., Burgath, K., and Wolff, F. (1977). Geologie und Petrologie des neogenen Kalkalkali Vulkanismus von Konya (Erenler Dağ-Alaca Dağ-Massiv, Zentral-Anatolien). *Geol. Jahrb.*, B25, 37–117.
- Koç, A., Kaymakci, N., van Hinsbergen, D. J. J., and Kuiper, K. F. (2017). Miocene tectonic history of the Central Tauride intramontane basins, and the paleogeographic evolution of the Central Anatolian Plateau. *Global Planet. Change*, 158, 83–102.
- Koç, A., Kaymakci, N., van Hinsbergen, D. J. J., Kuiper, K. F., and Vissers, R. L. M. (2012). Tectono-Sedimentary evolution and geochronology of the

- Middle Miocene Altınapa Basin, and implications for the Late Cenozoic uplift history of the Taurides, southern Turkey. *Tectonophysics*, 532–535, 134–155.
- Koç, A., van Hinsbergen, D. J. J., and Langereis, C. G. (2018). Rotations of normal fault blocks quantify extension in the Central Tauride intramontane basins, SW Turkey. *Tectonics*, 37(8), 2307–2327.
- Koçak, K. and Zedef, V. (2016). Geochemical Characteristics of the Lava Domes in Yatağan Village and Sağlık Town, From Erenlerdağı (Konya, Central Turkey) Volcanites. *Acta Geobalcanica*, 2(1), 7–19.
- Le Bas, M. J., Le Maitre, R. W., Streckeisen, A., and Zanettin, B. (1986). A chemical classification of volcanic rocks based on total alkali-silica diagram. *J. Petrol.*, 27(3), 745–750.
- Moix, P., Beccalotto, L., Kozur, H. W., Hochard, C., Rosselet, F., and Stampfli, G. M. (2008). A new classification of the Turkish terranes and sutures and its implication for the paleotectonic history of the region. *Tectonophysics*, 451(1–4), 7–39.
- MTA (2013). *Magmatic Rocks Map of Turkey*. General Directorate of Mineral Research and Explorations, Ankara.
- Okay, A. I. and Tüysüz, O. (1999). Tethyan sutures of Northern Turkey. In Durand, B., Jolivet, L., Hovarth, F., and Séranne, M., editors, *The Mediterranean Basins: Tertiary Extension within the Alpine Orogen*, pages 475–515. Geological Society, London.
- Özgül, N. (1976). Torosların Bazı Temel Jeoloji Özellikleri. *Türkiye Jeol. Kur. Bül.*, 19, 65–78.
- Özkan, A. M. and Söğüt, A. R. (1998). Dilekçi (Konya Batısı) Çevresindeki Neojen Çökellerinin stratigrafisi. *Mühendislik Bilimleri Dergisi*, 15(2–3), 1131–1138.
- Poznanović-Spahić, M., Marinković, G., Spahić, D., Sakan, S., Jovanić, I., Magazinović, M., and Obradović, N. (2023). Water-Rock interactions across volcanic aquifers of the lece andesite complex (Southern Serbia): geochemistry and environmental impact. *Water*, 15, article no. 3653.
- Robertson, A. H. F., Parlak, O., and Ustaömer, T. (2013). Late Palaeozoic-early Cenozoic tectonic development of southern Turkey and easternmost Mediterranean region: evidence from the interrelations of continental and oceanic units. In Parlak, O. and Ünlügenç, U. C., editors, *Geological Development of Anatolia and the Easternmost Mediterranean Region*, pages 9–48. Geological Society, Special Publications, London.
- Şahinci, A. (1991). *Doğal suların jeokimyası*. Reform Matbaası, İzmir.
- Schoeller, H. (1965). Qualitative evaluation of groundwater resources. In Schoeller, H., editor, *Methods and Techniques of Groundwater Investigations and Development*, pages 54–83. The United Nations Educational, Scientific and Cultural Organization, Paris.
- Şengör, A. M. C., Nalan, L., Gürsel, S., Cengiz, Z., and Taylan, S. (2019). The Phanerozoic palaeotectonics of Turkey. Part I: an inventory. *Mediterr. Geosci. Rev.*, 1, 91–161.
- Temel, A., Gündoğdu, M. N., and Gourgaud, A. (1998). Petrological and geochemical characteristics of Cenozoic high-K calc-alkaline volcanism in Konya, Central Anatolia, Turkey. *J. Volcanol. Geotherm. Res.*, 85(1–4), 327–354.
- Teng, H. H. (2005). Water-rock interactions. In Lehr, J. H. and Keeley, J., editors, *Water Encyclopedia*, page 846. John Wiley & Sons, New Jersey.
- Turan, A. (2010). Akören (Konya, Orta Toroslar) Çevresinin Jeolojik Özellikleri. *S.Ü. Müh.-Mim. Fak. Derg.*, 25(4), 17–36.
- Turan, A. (2020). Akkise-Yalılıyük (Konya) Arasının Stratigrafisi-Stratigraphy of Between Akkise and Yalılıyük (Konya). *DEÜ Mühendislik Fakültesi Fen ve Mühendislik Dergisi*, 22(64), 369–382.
- Wohletz, K. and Heiken, G. (1992). *Volcanology and Geothermal Energy*. University of California Press, Berkeley.
- Yidana, S. M., Banoeng-Yakubo, B., Aliou, A., and Akabzaa, T. M. (2012). Groundwater quality in some Voltaian and Birimian aquifers in Northern Ghana-application of multivariate statistical methods and geographic information systems. *Hydrol. Sci. J.*, 57(6), 1168–1183.
- Zhang, K., Deng, X., Gao, J., Liu, S., Wang, F., and Han, J. (2022). Insight into the process and mechanism of water-rock interaction in underground coal mine reservoirs based on indoor static simulation experiments. *ACS Omega*, 7(41), 36387–36402.